Collagen (I) homotrimer does not cause bone fragility but potentiates the osteogenesis imperfecta (oim) mutant allele

Katie J. Lee [a], Lisa Rambault [b], George Bou-Gharios [a], Peter D. Clegg [a, c], Riaz Akhtar [d], Gabriela Czanner [e], Rob van 't Hof [a], Elizabeth G. Canty-Laird [a, c]

[a] Department of Musculoskeletal and Ageing Science, Institute of Life Course and Medical Sciences, University of Liverpool, William Henry Duncan Building, 6 West Derby Street, Liverpool, L7 8TX, United Kingdom
[b] Université de Poitiers, France
[c] The Medical Research Council Versus Arthritis Centre for Integrated Research into Musculoskeletal Ageing (CIMA)
[d] Department of Mechanical, Materials and Aerospace Engineering, School of Engineering, University of Liverpool, L69 3GH, United Kingdom
[e] Department of Applied Mathematics, Faculty of Engineering and Technology, Liverpool John Moores University, Byrom Street, Liverpool, L3 3AF, United Kingdom

Abstract

Type I collagen is the major structural component of bone where it exists as an $(\alpha1)_2(\alpha2)_1$ heterotrimer in all vertebrates. The oim mouse model comprising solely homotrimeric $(\alpha1)_3$ collagen-1, due to a dysfunctional α2 chain, has a brittle bone phenotype implying that the heterotrimeric form is required for physiological bone function. However, humans with null alleles preventing synthesis of the α2 chain have connective tissue and cardiovascular abnormalities (cardiac valvular Ehlers Danlos Syndrome), without evident bone fragility. Col1a2 null and osteogenesis imperfecta (oim) mouse lines were used in this study and bones analysed by microCT and 3-point bending. RNA was also extracted from heterozygote tissues and allelic discrimination analyses performed using qRT-PCR. Here we show that mice lacking the α2(I) chain do not have impaired biomechanical or bone structural properties, unlike oim homozygous mice. However Mendelian inheritance was affected in male mice of both lines and male mice null for the α2 chain exhibited age-related loss of condition. The brittle bone phenotype of oim homozygotes could result from detrimental effects of the oim mutant allele, however the phenotype of oim heterozygotes is known to be less severe. We used allelic discrimination to show that the oim mutant allele is not downregulated in heterozygotes. We then tested whether gene dosage was responsible for the less severe phenotype of oim heterozygotes by generating compound heterozygotes. Data showed that compound heterozygotes had impaired bone structural properties as compared to oim heterozygotes, albeit to a lesser extent than oim homozygotes. Hence, we concluded that the presence of heterotrimeric collagen-1 in oim heterozygotes alleviates the effect of the oim mutant allele but a genetic interaction between homotrimeric collagen-1 and the oim mutant allele leads to bone fragility.

Key words: collagen, homotrimer, Col1a2, α2(I), osteogenesis imperfecta, cvEDS

Introduction

Type I collagen is the major structural component of vertebrate tissues, where it exists as insoluble fibrils formed from arrays of trimeric collagen molecules. In tetrapods, type I collagen molecules are predominantly $(\alpha1)_2(\alpha2)_1$ heterotrimers derived from the polypeptide gene products of the Col1a1 and Col1a2 genes. Trimeric type I procollagen molecules contain a central triple-helical domain flanked by globular N- and C-propeptide regions, that are proteolytically removed to facilitate fibrillogenesis (Canty and Kadler, 2005). Procollagen molecules are synthesised in the endoplasmic reticulum of the secretory pathway where individual molecules first associate via the C-propeptides. C-propeptide association facilitates chain registration and folding of the triple helical domain into a right-handed triple helix. The type-specific assembly of fibrillar procollagens has been attributed to defined amino acid sequences within the C-propeptide including a chain recognition sequence (Lees et al., 1997), specific stabilising residues (Sharma et al., 2017) and a cysteine code (DiChiara et al., 2018), although none fully explain the preferential heterotrimerisation of type I procollagen.

Abnormal type I collagen $(\alpha1)_3$ homotrimer, derived from COL1A1 alone, is genetically or biochemically associated with common age-related human diseases including osteoporosis (Ralston et al., 2006), osteoarthritis (Bailey et al., 2002; Kerns et al., 2014; Philp et al., 2017), intervertebral disc degeneration (Zhong et al., 2017), arterial stiffening (Brull et al., 2001), cancer (Makareeva et al., 2010), liver fibrosis (Rojkind et al., 1979) and Dupuytren's contracture (Ehrlich et al., 1982). The homotrimeric form is resistant to mammalian collagenases (Han et al., 2010) and alterations in collagen crosslinking have been reported in the osteogenesis imperfecta murine (oim) model, which lacks a functional α2(I) chain (Carriero et al., 2014; Pfeiffer et al., 2005; Sims et al., 2003). Hence the presence of homotrimeric collagen (I) in human disease may alter the ability of tissues to respond to changing physiological demands by slowing remodelling and altering tissue mechanics.

The oim mutation is a deletion of a single guanidine residue, causing a frameshift that alters the last 47 amino acids and adds an additional residue to the α2 chain of type I procollagen (Fig. 1A). The mutant α2 chain cannot be incorporated into trimers hence giving rise to solely homotrimeric collagen-1 in oim homozygotes. Homozygous oim/oim mice have osteopenia, progressive skeletal deformities, spontaneous fractures, cortical thinning and small body size (Chipman et al., 1993) with corresponding alterations to bone structure and material properties. (Carleton et al., 2008; Grabner et al., 2001). Homozygous oim mice also have a reduced circumferential breaking strength and greater compliance of aortae (Pfeiffer et al., 2005; Vouyouka et al., 2001), reduced ultimate stress and strain tendon for tendon (Misof et al., 1997) and kidney glomerulopathy (Phillips et al., 2002).

The oim mutation is very similar to the first-identified mutation causing human osteogenesis imperfecta (autosomal recessive Silence type III), in which a 4 nucleotide deletion (c.4001_4004del) causes a frameshift (p.(Asn1334Serfs*34)) to alter the last 33 amino acids of the α2 chain of type I procollagen (Pihlajaniemi et al., 1984). The human mutation also results in homotrimeric type I collagen synthesis as the defective α2(I) chain cannot be incorporated into trimers (Nicholls et al., 1984; Nicholls et al., 1979). In two additional patients with mild osteogenesis imperfecta, novel mutations were identified causing a 48 amino acid truncation of the α2 chain and a substitution of a cysteine residue important for interchain disulphide bonding respectively (Pace et al., 2008). In these cases the α2 chain was again synthesised but not incorporated into trimers. A similar mutation causing severe osteogenesis imperfecta in a Beagle dog was caused by a heterozygous 9 nucleotide

replacement of a 4 nucleotide stretch, leading to a 37 residue truncation of the α2 chain and alteration of the final 44 amino acids of the truncated polypeptide (Campbell et al., 2001).

Oim heterozygotes do not show spontaneous fractures but appear to have a bone phenotype intermediate between that of wild-type and homozygous mice (Camacho et al., 1999; Grabner et al., 2001; Saban et al., 1996; Yao et al., 2013). Similarly the parents of the human proband had no history or evidence of fractures but had a marked decrease in bone mass (Prockop, 1988).

The osteogenesis imperfecta brittle bone phenotype contrasts with the phenotype of human patients in which mutations leading to nonsense-mediated decay of the COL1A2 mRNA cause a specific cardiac valvular form of Ehlers-Danlos syndrome (cv-EDS) (Guarnieri et al., 2019; Malfait et al., 2006). EDS is generally characterised by hyperextensible skin and joint hypermobility. In cv-EDS patients the α2 chain of type I collagen is not synthesised, therefore all type I collagen molecules would be homotrimeric. It has been hypothesised that the phenotypic differences between the patients could be explained by the cellular stress elicited by the presence of misfolded α2(I) procollagen chains in osteogenesis imperfecta (Forlino et al., 2011; Makareeva et al., 2011; Pace et al., 2008), having a particularly detrimental effect on bone. Cellular stress has been implicated in human osteogenesis imperfecta caused by substitutions in the C-propeptide of the α-1(I) chain (Chessler and Byers, 1993), in mouse models of triple-helical region mutations; Aga2 (90 a.a. extension to the α1(I) chain) (Lisse et al., 2008), Brtl IV (G349C in α1(I)) (Forlino et al., 2007) and Amish (G610C in α2(I)), identical to that found in a human kindred) (Mirigian et al., 2016), as well as in the zebrafish model Chihuahua (G574D in α1(I)) (Gioia et al., 2017).

In this study we compared the bone phenotype of the oim model to that of a Col1a2 null mouse. We considered that comparing the oim model to that of a Col1a2 null line provided a unique opportunity to distinguish between the intracellular and extracellular effects of a collagen mutation linked to brittle bone disease, as well as to elucidate the effect of collagen (I) homotrimer on bone structure and biomechanics. Specifically, we compared the bone phenotype of oim homozygous and heterozygous mutant mice with that of mice containing 1 or 2 copies of a targeted Col1a2 null allele and wild-type controls, in order to determine the contribution of collagen (I) homotrimer to bone fragility.

Materials and Methods

Mouse models

A Col1a2 knock-out mouse line ($Col1a2^{tm1b(EUCOMM)Wtsi}$, C57BL/6N) (Col1a2 null, N) and osteogenesis imperfecta mouse line ($Col1a2^{oim}$, C57BL/6J) (oim, J) were used to investigate the effects of the absence and the mis-folding of the α2(I) polypeptide chain respectively (Fig. 1B). The $Col1a2^{tm1b(EUCOMM)Wtsi}$ line was derived from $Col1a2^{tm1a(EUCOMM)Wtsi}$, purchased from the Mutant Mouse Resource and Research Centre (MMRRC) at UC Davies, by Cre-mediated recombination (Skarnes et al., 2011) during IVF provided by MRC Harwell. The $Col1a2^{oim}$ line was a kind gift from Prof. Charlotte Phillips, University of Missouri and was subsequently rederived using Charles River (Massachusetts, USA) services. Mice were housed at the University of Liverpool in a specific pathogen free unit in groups of up to 5 by litter, with oim homozygotes and Col1a2 null/oim heterozygotes housed separately after weaning. Food and water were supplied *ad libitum* and wet food was supplied to oim homozygotes and Col1a2 null/oim heterozygotes due to fragile teeth. Cage balconies were

removed for oim homozygotes and Col1a2 null/oim heterozygotes to reduce fracture risk and non-tangling bedding was supplied as standard for all mice. The mice were housed at 20-24°C and 45-65% humidity with a 12 hour light/dark cycle. All breeding and maintenance of animals was performed under project licences PP4874760 and P92F55CB2, in compliance with the Animals (Scientific Procedures) Act 1986 and UK Home Office guidelines. Details of all animals were recorded on tick@lab (a-tune) laboratory animal management software (Darmstadt, Germany), including health and treatment reports. Genotyping was carried out using Transnetyx (Tennessee, USA) services using the 'Col1a2-2 WT' probe with 'LAC Z' or 'L1L2-Bact-P TA' for tm1a allele or 'L1L2 tm1b' for tm1b allele, and the 'oim' probe for the oim line. Blinding was carried out by processing mice and labelling samples according to the mouse number, rather than genotype. Wild-type (N +/+, J +/+), heterozygote (N +/-, J +/oim) and homozygote (N -/-, J oim/oim) mice were sacrificed at 8 (±3 days) and 18 (±3 days) weeks for analysis as well as 52 weeks (±8 days) for the Col1a2 null line. Eight and 18 weeks were chosen as the time points at which long bone growth and bone mineralisation respectively are complete. Oim mice were not maintained up to 52 weeks due to welfare considerations for homozygotes exhibiting spontaneous fractures. Cross-breeding of both lines was also performed (Col1a2 null/oim, mixed background) and wild-type (+/+), Col1a2 null heterozygote (+/oim), oim heterozygote (+/-) and compound heterozygote (-/oim) mice were sacrificed at 8 weeks.

Mouse dissection

Mice were culled using a rising carbon dioxide concentration method in an automated CO_2 delivery chamber. After confirmation of the permanent cessation of the circulation, the mice were weighed and the tail was removed at the base and added to PBS for further dissection. Next, the skin was removed, the femoral heads displaced from the acetabulum and the entire hind limbs detached and added to PBS. The skin was then removed from the tail and the tail tendons dissected free. Excess muscle was removed from the hind limbs and the feet removed at the tarsus. For techniques requiring isolated tendon and bone tissue, the patellar tendon was further removed, the femur and tibia separated, and all muscle dissected out.

Pulse-chase with ^{14}C-L-proline

Tail tendon, patellar tendon and femur tissue was dissected from 8 week old Tm1b mice. Tissue was dissected into small pieces and added to DMEM containing penicillin/streptomycin (1% v/v), L-glutamine (2 mM), L-ascorbic acid 2-phosphate (200 µM), β-aminopropionitrile (400 µM) and 2.5 µCi/ml [^{14}C]proline (GE Healthcare) and incubated at 37°C for 18 hours. The tissue samples were subsequently moved to media without [^{14}C]proline for 3 hours. Collagen was then extracted from the tissue samples using a salt extraction buffer (1 M NaCl, 25 mM EDTA, 50 mM Tris-HCl, pH 7.4) containing protease inhibitors (Roche, Basel, Switzerland). Samples were extracted overnight at 4°C with agitation. Extracts were analysed by electrophoresis on 6% Tris-Glycine gels (ThermoFisher, Massachusetts, USA)) with delayed reduction (Sykes et al., 1976). The gels were fixed (10% methanol, 10% acetic acid), dried under vacuum, and exposed to a phosphorimaging plate (BAS-IP MS). Phosphorimaging plates were processed using a phosphorimager (Typhoon FLA7000 IP) and densitometry carried out using ImageQuant software (GE Healthcare Life Sciences, Illinois, USA).

Three point bending

Before three-point bending tests, the freshly isolated intact femurs and tibias (only those showing no evidence of fracture calluses) were imaged using uCT in order to obtain the cross-sectional area, circumference and moment of inertia measurements. Bones were scanned inside 1 ml syringes in PBS using a Skyscan 1272 scanner (Bruker, Kontich, Belgium). Scans were performed at a resolution of 9 µm (60 kV, 150 µA, 2x2 binning, rotation step size 0.5°, using a 0.5 mm aluminium filter). Scans were reconstructed using NRecon (Bruker) using Gaussian smoothing of 1, ring artefact reduction 5, and beam hardening compensation at 38%. For analysis of cortical bone parameters, a region of interest of 200 slices of the mid-femur and mid-tibia was selected and saved using Dataviewer (Bruker). Cross-sectional area, circumference and moment of inertia as well as bone density measurements were obtained using a custom macro in CTan (Bruker). Density measurements were calibrated using a set of hydroxyapatite phantoms (Bruker, Kontich, Belgium).

A Zwickiline Fmax 1 kN (Zwick, Ulm, Germany) biomechanical tester fitted with a 50N load cell was used for three-point bending experiments. Femurs and tibias were loaded at a span length of 8 mm and the crosshead was lowered at a rate of 0.5 mm/min using testXpert II software (Zwick). Ultimate force and stiffness measurements were calculated from the force-displacement curve, at the point of maximum load and the maximum gradient of the linear rising section of the graph respectively. The maximum stiffness was calculated using equation 1.1 and elastic modulus by equation 1.2.

Eq. 1.1 Stress = ultimate force x ((span x radius) / 4 x moment of inertia))

Eq. 1.2 Elastic modulus = (stiffness x span)^3 / 48 x moment of inertia

Micro computed tomography (uCT)

Hind limbs were fixed overnight in 10% neutral buffered formalin before washing and storage in 70% ethanol. Limbs were loaded into 2 ml syringe tubes in 70% ethanol and scanned using a Skyscan 1272 scanner (Bruker, Kontich, Belgium) at a resolution of 4.5 µm(60 kV, 150 µA, no binning, rotation step size 0.3°, using a 0.5 mm aluminium filter). Scans were reconstructed using NRecon software (Bruker) as described above. Trabecular bone parameters of the proximal tibia were measured in a volume, selected and saved using Dataviewer (Bruker), of 200 slices starting 20 slices distal to the growth plate as described {van 't Hof, 2019 #3510. As previously, only bones that did not contain any fracture calluses were used. Trabecular bone parameters were measured using a custom macro in CTan (Bruker).

Allelic discrimination

RNA was extracted from tissues preserved in RNAlater by firstly applying Trizol to samples which were then homogenised using a steel ball lysing matrix and a FastPrep 24 tissue homogeniser (MP Biomedicals, California, USA). RNA was extracted from homogenised samples using a Direct-Zol RNA kit (Zymo Research, California, USA) as per the manufacturer's instructions. The quantity and quality of RNA was assessed using a NanoDrop spectrophotometer (Thermo Fisher), 260/280 values between 1.8-2.1 were deemed of a sufficient RNA quality. cDNA was synthesised in a 25 µl reaction from 0.5-1 µg of total RNA. The conditions for cDNA synthesis were: incubation at 5 minutes at 70°C, 60 minutes at 37°C and 5 minutes at 93°C with 1 U/µl RNasin ribonuclease inhibitor, 2 mM PCR nucleotide mix, 8 U/µl M-MLV reverse transcriptase and 0.02 µg/µl random-hexamer oligonucleotides per reaction.

Detection of murine Col1a2 wild-type and mutant alleles was performed using a custom snpsig™ real-time PCR mutation detection/allelic discrimination kit (Primerdesign, Southampton, UK). 10 ng of cDNA was added to 10 µl of PrecisionPLUS mastermix (Primerdesign), 1 µl of the custom genotyping primer/probe mix and 4 µl nuclease free water per reaction. Amplification was performed on a Stratagene qPCR machine with an initial enzyme activation step of 2 minutes at 95°C followed by 10 cycles of denaturation for 10 seconds at 95°C and extension for 60 seconds at 60°C. Finally, 35 cycles of denaturation for 10 seconds at 95°C and extension for 60 seconds at 68°C, with fluorogenic data collected during this extension step for the ROX (wild type) and VIC (oim) channels.

Statistical analysis

Sample size calculations were carried out using G*Power 3.1.9.2 and Stata13 to give a power of at least 90% at the 5% level of significance. Primary outcomes were defined as bone stiffness (N/mm), bone volume (%) and trabecular separation (µm) with a standardised effect size of 2 deemed to be biologically important. For comparison, effect sizes were calculated from previously reported oim data (Vanleene et al., 2011) as -2.0 (41%) for femur stiffness, -2.8 (48%) for bone volume and 2.8 (66%) for trabecular separation. Comparison of 'bone mineral density' (DEXA) effect sizes for the oim (Phillips et al., 2000) and Col1a2 null lines (IMPC) at 14 wks indicated effect sizes of a similar magnitude (d=-1.6 and 1.7 respectively). Group sizes of 3 were calculated for two-way ANOVA on normally distributed data to test the effect of genotype (Stata13). The sample size in each group was increased by 20% to allow for non-normality of the data to give planned group sizes of 4.

All statistical analysis was completed using SigmaPlot software. Comparisons of continuous measurements across sex and genotype were carried out using a two-way ANOVA with a Holm-Sidak post-hoc test. Continuous data failing a Shapiro-Wilk test were transformed using LOG10 transformation prior to analysis. For continuous data still failing a Shapiro-Wilk test after transformation a nonparametric Kruskal-Wallis H test on ranks with a Dunn's post-hoc test was used for comparisons. Comparisons of two categorical variables were done via a Chi-squared test with the expected counts in each cell of the table being at least 5. The time to deterioration data were summarised via survival curves and statistically compared via a log-rank (Mantel-Cox) test, overall p-value is reported. Data were plotted using GraphPad Prism 8.

Results

Tm1b homozygotes lack the α2(I) collagen chain in bone and tendon

To verify lack of the α2(I) chain in tm1b homozygotes, tendon and bone samples from 8 week old mice were labelled with [14C]proline to detect newly synthesised collagen (I). SDS-PAGE analysis of labelled tissue extracts verified lack of α2(I) chain synthesis in tail tendon, bone and patellar tendon (Fig. 1C).

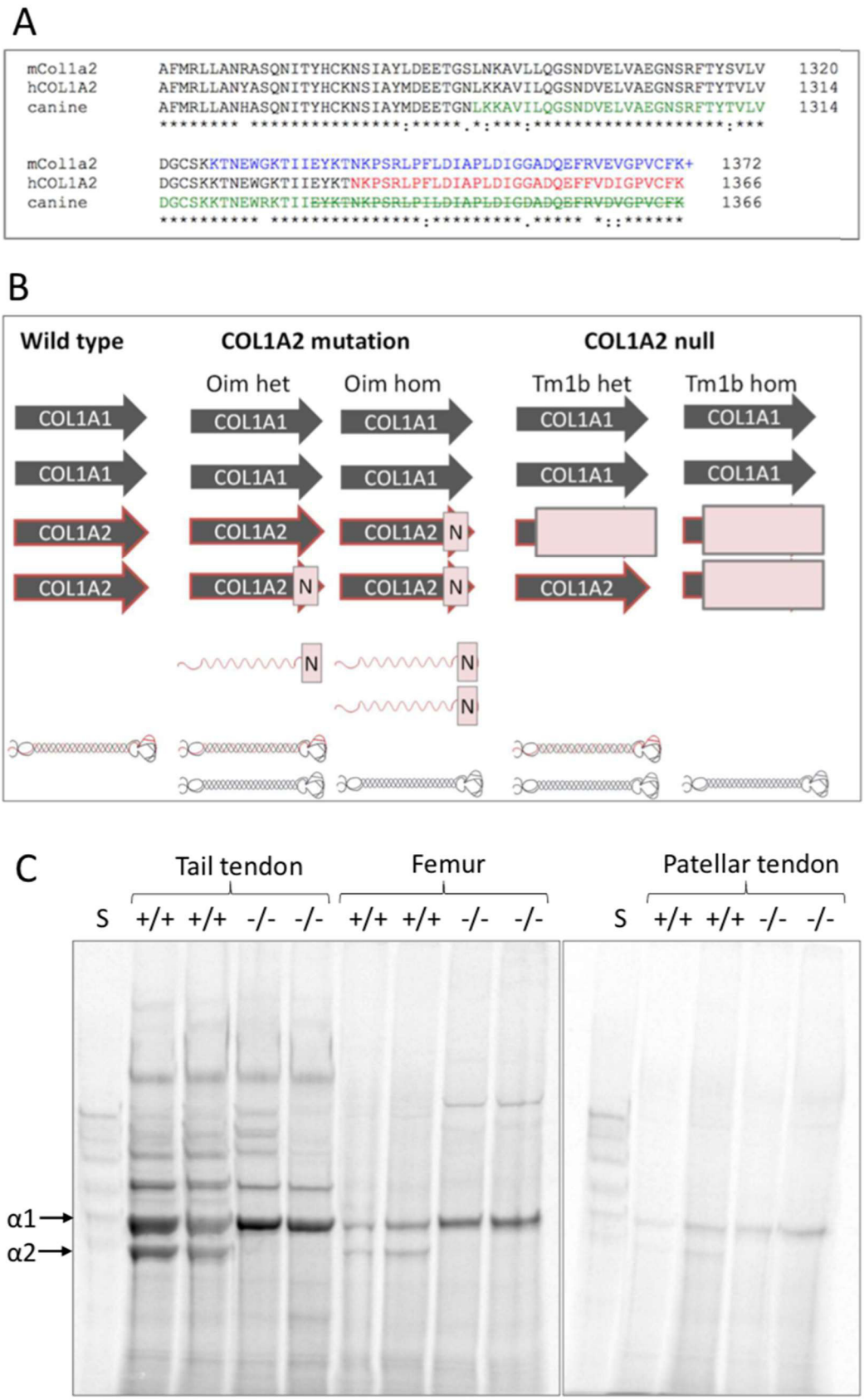

Figure 1. Col1a2 mutant and null alleles. A: Amino acid sequence alignment for the final 112 residues of the mouse (mCol1a2), human (hCOL1A2) and canine α2(I) collagen chains. Colour change

indicates amino acid sequence changed from that shown due to frameshift caused by the oim or equivalent mutation. + indicates additional amino acid. Strike-through indicates truncation. B: Genetic differences between the oim and Col1a2 null lines with implications for collagen (I) protein synthesis. Arrows indicate COL1 genes; N indicates mutation, light red box indicates null allele. Folded heterotrimeric proteins are indicated in black and red, whilst homotrimers are in black only. The presence of unincorporated mutant Col1a2 allele is indicated as a red waveform with a mutation (N). C: Tendon and bone tissue from Tm1b wild-type (+/+) and homozygote (-/-) mice were labelled with [14C]proline and analysed by delayed reduction SDS-PAGE. No labelled α2(I) chain was present in tm1b homozygotes (-/-) unlike in wild-type controls (+/+) indicating that tm1b homozygotes are Col1a2 null. S; collagen standard. α1(I) and α2(I) chains are indicated.

Alterations to Mendelian inheritance in male mice of the oim and Col1a2 null lines

To determine if either the oim or Col1a2 alleles resulted in loss of mice prior to weaning, a chi-squared test was performed on genotype data for Col1a2 null and oim mice. There were significant differences between the observed and expected genotype percentages for male mice of both lines (oim; p=0.01, Col1a2 null; p=0.033), whereas no differences were seen for female mice of either line (Fig. 2 A-B). The data supported Mendelian inheritance in female mice, whereas increased numbers of male wild-types and reduced numbers of male heterozygotes were observed for both lines. A small reduction in the numbers of male homozygous oim mice was noted.

Spontaneous fractures were observed solely in oim homozygotes, whilst male Col1a2 null homozygotes exhibited mild joint swelling.

During colony maintenance it was noticeable that spontaneous fractures occurred in the oim line, but not in the Col1a2 null line. Mildly swollen ankle joints were however observed in male tm1b mice which was initially attributed to fighting. The proportion of mice with swollen joints, or noticeable fractures with swelling were determined, including those requiring analgesia (Fig. 2 C-D). Male mice demonstrated a more severe phenotype than female mice for both the Col1a2 null and oim lines. For the oim line fractures and associated swelling were observed in homozygous mice only, with an incidence of 47% for males (20 out of 43) and 20% (10 out of 50) for females. 26% of male mice (11 out of 43) and 18% of female mice (9 out of 50) received analgesic medication. Swollen joints alone presented in 6% of male oim heterozygotes (5 out of 89), 2% of male oim homozygotes (1 out of 43) and 2% of female oim homozygotes (1 out of 50). For the Col1a2 null line no bone fractures were observed and no analgesia was required to be administered. Swollen joints were observed predominantly in male homozygotes with an incidence of 23% (19 out of 83). Less than 4% of male wild-type (4 out of 103), heterozygous (4 out of 126) and female homozygous (1 out of 56) mice presented with swollen joints. No female wild-type or heterozygous mice were reported to have swollen joints. For mouse weights recorded after euthanasia at 18 weeks, male oim homozygotes were significantly lighter than wild-types (p=<0.001) and heterozygotes (p=<0.001), whilst female wild-types were significantly heavier than heterozygotes (p=0.024) and homozygotes (p=<0.001) (Fig. 2E). In contrast, there was no difference in weight between genotypes for the Col1a2 null line (Fig. 2F).

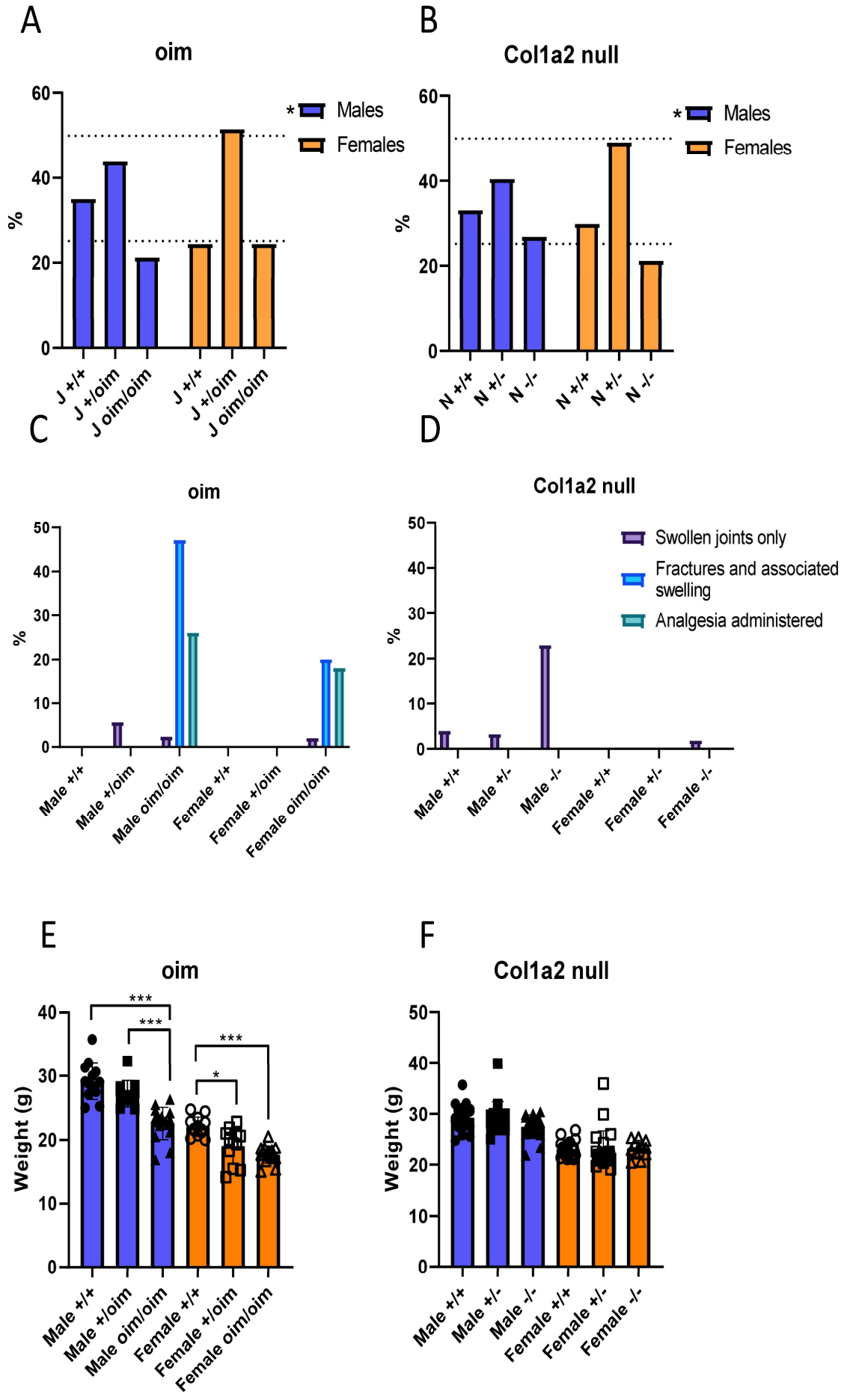

309

Figure 2. Inheritance pattern, musculoskeletal health summary and mouse weights for the oim and Col1a2 null lines. A-B: The percentage of mice of each genotype born to heterozygous parents for the oim (A) and Col1a2 null (B) lines. A chi-squared test showed significant differences between observed and expected inheritance for male mice of both lines. C-D: The number of mice suffering from swollen joints and bone fractures as well as those treated with analgesics were recorded for the oim (C) and Col1a2 null (D) lines. These numbers are expressed as a percentage of total mouse numbers. A-D: n=71, 89 and 43 for male oim +/+, +/oim and oim/oim mice respectively; n=50, 106 and 50 for female oim +/+, +/oim and oim/oim mice respectively; n= 103, 126 and 83 for male Col1a2 null +/+, +/-, -/- mice respectively and; n=79, 130, 56 for female Col1a2 null +/+, +/-, -/- mice respectively. Swollen joints were mild in the Col1a2 null line and often not noted until advanced age, therefore the numbers shown above may be an underestimation due to many mice being culled at earlier time points. E-F: Weights of 18 week oim (E) and Col1a2 null (F) mice measured after euthanasia. Blue bars/filled shapes = males, orange bars/open shapes = females. * = p-value < 0.05 and *** = p-value <0.001. E: p-value for genotype <0.001 for males and females. E-F: n= 13, 11 and 16 for male oim male +/+, +/oim and oim/oim mice respectively, n=13, 12 and 15 for female oim +/+, +/oim and oim/oim mice respectively, n= 21, 17 and 17 for male Col1a2 null +/+, +/-, -/- mice respectively, n=21, 22, 12 for female Col1a2 null +/+, +/-, -/- mice respectively.

Three-point bending of bones from oim and Col1a2 null mice

To determine whether extrinsic and intrinsic biomechanical properties of bones differed between the Col1a2 null and oim lines, femurs and tibias from both male and female mice at various ages were subjected to three-point bending to measure strength, stiffness, stress and elastic modulus (Figs. 3&4).

Generally, at 8 weeks of age, bones from oim homozygote animals showed a reduction in strength. Femurs from oim male homozygotes showed a 47% and 43% decrease in strength (Fig. 3A) and stiffness (Fig. 3B) respectively compared with wild-type controls, heterozygotes also demonstrated a decrease in strength and stiffness compared to wild-type controls, however these differences were not significant. A similar trend was seen in tibias from both males and females (Fig. 4 A&B), however, this was not statistically significant. Ultimate strength was also reduced by 50% in femurs from homozygote females at this age (Fig. 3A), however, stiffness was not. There were no significant differences in stress, elasticity or bone cross-sectional area between oim genotypes at 8 weeks of age (Fig.3&4 C-E).

At 18 weeks of age, there were no statistically significant differences in 3-point bending parameters of the femur between the oim genotypes for female mice. However, ultimate stress was significantly reduced by 65% in 18-week-old oim male homozygous compared to heterozygous or wild-type femurs, whilst elastic modulus was 65% lower in oim homozygous than heterozygous femurs, and 52% lower than wild-types (Fig.3 H&I). In the tibia ultimate strength, stiffness and cross sectional area were significantly reduced in both male and female mice at this age. Although there was a trend for ultimate strength and stiffness of the femur to be reduced as well, this was not statistically significant (Fig.3 F, G).

Surprisingly, deletion of Col1a2 had only modest effects on 3-point bending parameters, and only the ultimate strength and ultimate stress (in males at 18 weeks of age) and elastic modulus (in males and females at 52 weeks of age) were affected. Ultimate strength of the tibia was decreased by 35% in homozygous males compared to wild-type males (Fig. 4F), whilst ultimate stress was

355 decreased by 39% in homozygous as compared to heterozygote males (Fig.4H). Elastic modulus was
356 increased by 38% in femurs from 52-week-old female Col1a2 null heterozygotes compared to
357 homozygotes (Fig.3N), and increased by 24% in tibia of female heterozygotes compared to wild-type
358 mice (Fig.4N). The elastic modulus was decreased by 26% in tibias from male Col1a2 null mice
359 compared to WT mice at 52 weeks (Fig.4N).
360 Whilst the strain of the lines differs slightly (C57BL/6J versus C57BL/6N) similar trabecular
361 bone parameters have been reported in both strains (Simon et al., 2013) and we observed no
362 significant differences between wild-types of either strain. Results across lines are therefore
363 comparable. For femur, oim heterozygotes had a significantly increased elastic modulus compared
364 to Col1a2 null heterozygotes at 18 weeks (Fig.3I). Tibias from 8 week old mice showed increased
365 stiffness in Col1a2 null male homozygotes compared to oim male homozygotes (Fig 4B). Stiffness
366 was also reduced in oim heterozygotes and homozygotes compared to the Col1a2 null equivalents
367 (Fig.4G). Cross-sectional area was reduced in oim homozygotes compared to Col1a2 null
368 homozygotes. There were no significant differences in strength, stiffness, stress and bone cross-
369 sectional area between genotypes at 52 weeks (Fig.4. K-M, O).
370

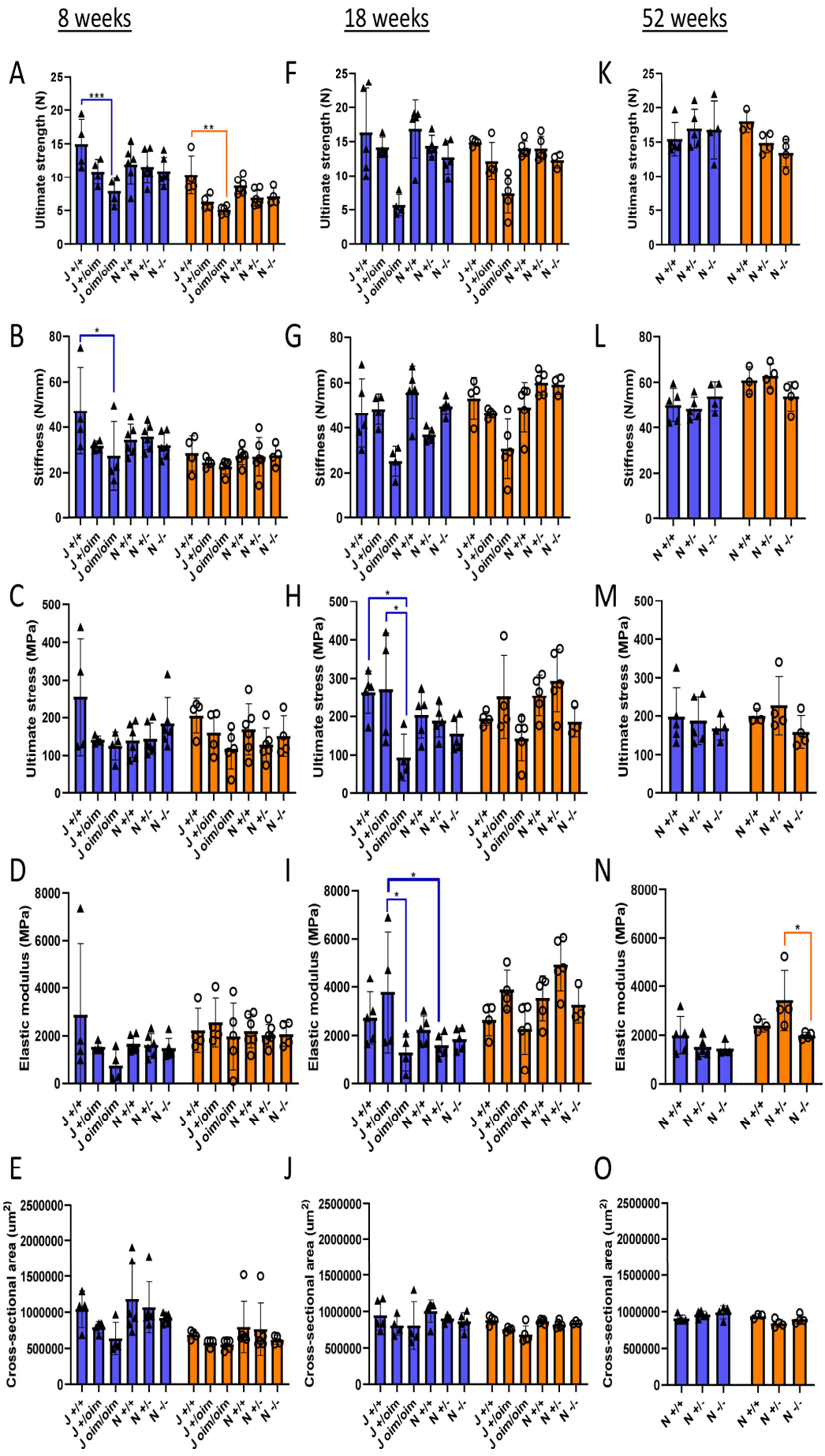

371

Figure 3. Three-point bending of femurs from oim and Col1a2 null mice. Femurs from oim and Col1a2 null mice were subjected to three-point bending at 8 (A-E), 18 (F-J) and 52 weeks (K-O). Ultimate strength (A, F, K) and stiffness (B, G, L) (extrinsic) measurements were normalised to cross-sectional area (E, J, O) to calculate ultimate stress (C, H, M) and elastic modulus (D, I, N) (intrinsic). Blue bars/triangles = males, orange bars/circles = females. Thin blue and orange bars show differences between genotypes and thick blue and orange bars show differences between mouse lines. * = p-value < 0.05, ** = p-value <0.01 and *** = p-value <0.001.Overall significant p-values from two-way ANOVA tests were <0.001 (genotype) and <0.001 (sex) for A, 0.043 (genotype) and <0.001 (sex) for B, 0.018 (genotype) for C, 0.001 (genotype) for H, 0.007 (genotype) and <0.001 (sex) for I, 0.004 (sex) for L, 0.1 (genotype) and <0.001 (sex) for N, 0.018 (sex) for O, whilst the overall p-values from Kruskall Wallis H tests were <0.001 for E, 0.003 for F and <0.001 for G. n=4 for all oim groups, except female J oim/oim and male 18 week J+/+ where n=5. n=6 for all Col1a2 null groups at 8 weeks and n=5 for all Col1a2 null groups at 18 weeks. n=4 for all Col1a2 null groups at 52 weeks, except female +/- and male +/+ where n=5 and male +/- where n=6.

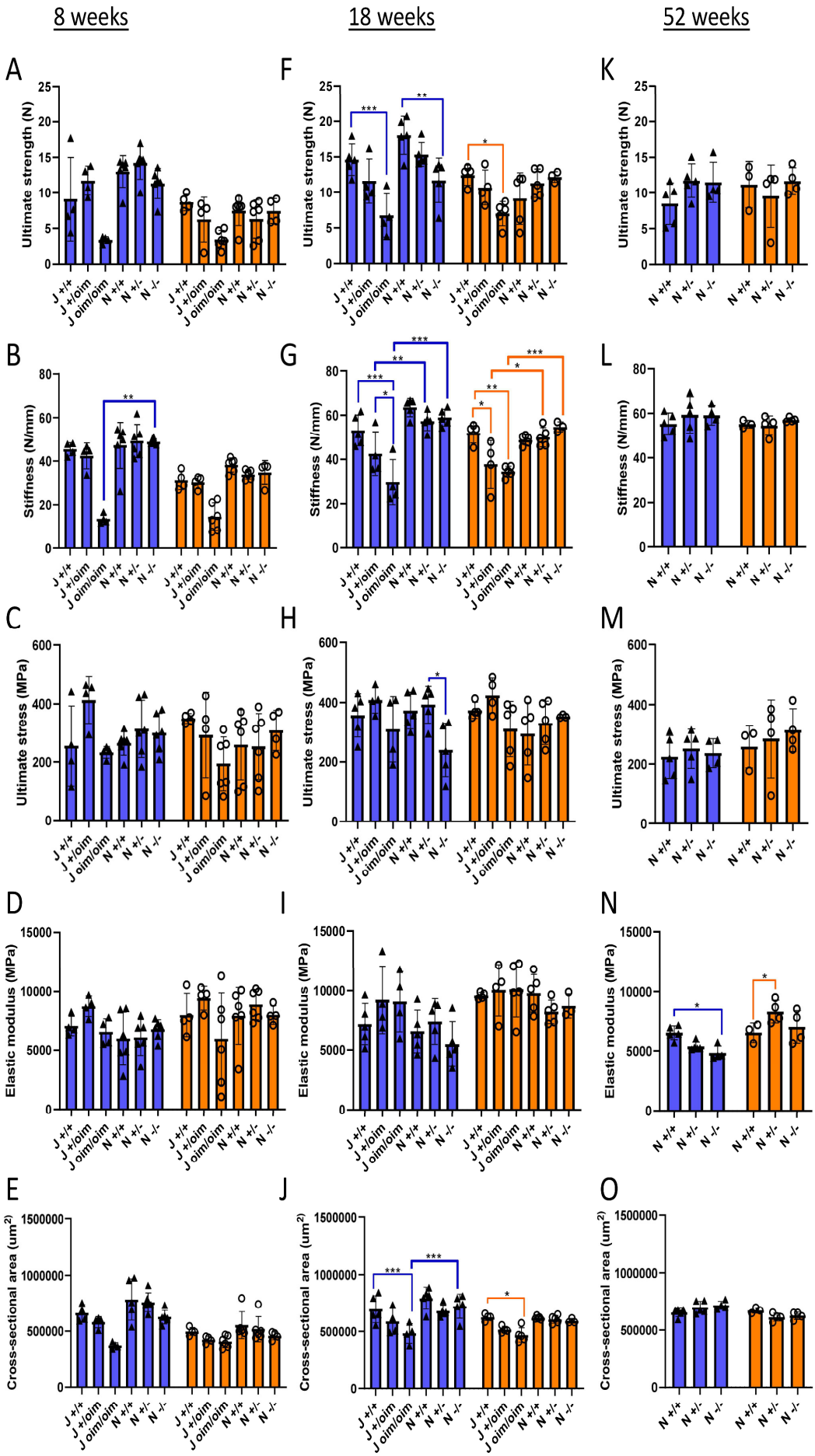

Figure 4. Three-point bending of tibias from oim and Col1a2 null mice. Tibias from oim and Col1a2 null mice were subjected to three-point bending at 8 (A-E), 18 (F-J) and 52 weeks (K-O). Ultimate strength (A, F, K) and stiffness (B, G, L) (extrinsic) measurements were normalised to cross-sectional area (E, J, O) to calculate ultimate stress (C, H, M) and elastic modulus (D, I, N) (intrinsic). Blue bars/triangles = males, orange bars/circles = females. Thin blue and orange bars show differences between genotypes and thick blue and orange bars show differences between mouse lines. * = p-value < 0.05, ** = p-value <0.01 and *** = p-value <0.001. Overall significant p-values from two-way ANOVA tests were <0.001 (genotype) and <0.001 (sex) for F, <0.001 (genotype) and 0.009 (sex) for G, 0.036 (genotype) for H, <0.001 (sex) for I, <0.001 (genotype) and <0.001 (sex) for J, 0.094 (genotype) and <0.001 (sex) for N, 0.003 (sex) for O, whilst the overall p-values from Kruskall Wallis H tests were p<0.001 for A, <0.001 for B, 0.018 for D, <0.001 for E. n=4 for all oim groups, except female 18 week oim/oim and male 18 week J+/+ where n=5, and female 8 week oim/oim where n=6. n=6 for all Col1a2 null groups at 8 weeks and n=5 for all Col1a2 null groups at 18 weeks. n=4 for all Col1a2 null groups at 52 weeks, except male +/+ where n=5 and male +/- where n=6.

Micro-computed tomography bone scans of oim and Col1a2 null mice

To analyse differences in bone structure between genotypes, the proximal tibias from oim and Col1a2 null mice were analysed by µCT (Fig. 5).

There were significant changes in bone volume and architecture in mice (both males and females) carrying the oim mutation at both 8 weeks and 18 weeks of age, and most of the differences showed an apparent gene dose effect. In males at 8 weeks, BV/TV was decreased by 42% in heterozygote mice and 80% in homozygous mice compared to wild-type controls (Fig. 5A), due to a decrease in both trabecular thickness (Fig. 5B) and trabecular number (Fig. 5D).The decrease in trabecular thickness and number lead to a 60% increase of trabecular separation in oim/oim homozygotes (Fig.5C). In addition, TMD was decreased by 21% in homozygous 8-week-old males compared to wild-type controls (Fig 5F), and although a similar trend was observed in heterozygote males, this was not statistically significant. Similar changes were observed in female mice at 8 weeks, however, the differences tended to be smaller, and the effect of the oim mutation was only statistically significant for BV/TV and trabecular number (Fig.5 A,D).

At 18 weeks of age, the pattern of the effects of the oim mutation on trabecular bone were similar to those observed at 8 weeks, however, the differences between WT mice and +/oim and oim/oim mice were generally smaller. For instance, BV/TV in males was decreased by 50% at 18 weeks (Fig. 5G), compared to 80% at 8 weeks of age (Fig. 5A). There were no differences in tissue mineral density at 18 weeks of age (Fig. 5L).

The effects of Col1a2 deletion on bone volume and architecture were relatively minor, and almost only observed in male mice at 8 weeks of age. The main difference was a 17% decrease in BV/TV in homozygote null mice compared to wild-type controls (Fig. 5A), associated with a 11% decrease in trabecular thickness (Fig. 5B), and a 8% decrease in trabecular number (Fig. 5D). In addition, male heterozygous null mice showed a 19% increase in TMD at 18 weeks of age (Fig. 5L), and homozygous null males showed a 22% increase in TMD at 52 weeks of age (Fig. 5R) compared to wild-type controls. Apparent gene-dosage dependent increases in BV/TV, trabecular number and connectivity were observed for male mice at 52 weeks.

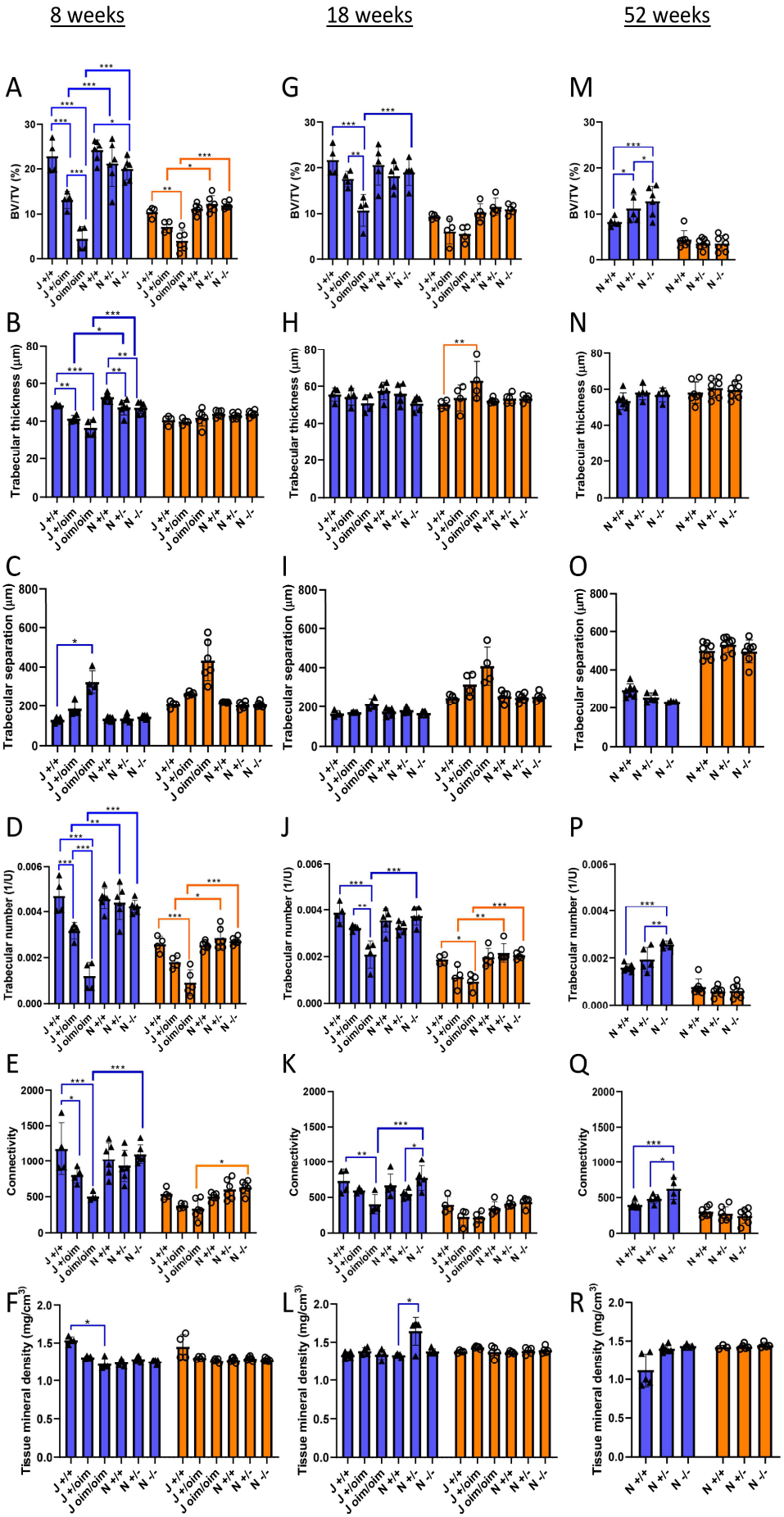

433

Figure 5. Micro-computed tomography bone scans of oim and Col1a2 null mice. MicroCT scans were performed on the knee joints of oim and Col1a2 null mice at 8 (A-F), 18 (G-L) and 52 weeks (M-R). Reconstruction and analysis of scan files enabled determination of bone volume (A, G, M), trabecular thickness (B, H, N), trabecular separation (C, I, O), trabecular number (D, J, P), connectivity (E, K, Q) and bone density(F, L, R). Blue bars/triangles = males, orange bars/circles = females. Thin blue and orange bars show differences between genotypes and thick blue and orange bars show differences between mouse lines. * = p-value < 0.05, ** = p-value <0.01 and *** = p-value <0.001. Overall p-values from two-way ANOVA tests were <0.001 (genotype) and <0.001 (sex) for A, <0.001 (genotype) and <0.001 (sex) for B, <0.001 (genotype) and <0.001 (sex) for D, <0.001 (genotype) and <0.001 (sex) for E, <0.001 (genotype) and <0.001 (sex) for G, 0.387 (genotype) for H, <0.001 (genotype) and <0.001 (sex) for J, <0.001 (genotype) and <0.001 (sex) for K, 0.004 (genotype) and <0.001 (sex) for M, <0.001 (genotype) for O, 0.007 (genotype) and <0.001 (sex) for P, 0.075 (genotype) and <0.001 (sex) for Q, and the overall p-values from Kruskall Wallis H tests were <0.001 for C, <0.001 for F, <0.001 for I, 0.014 for L, 0.015 for R. n=4 for all oim groups, except female 8 week old oim/oim where n=6. n=6 for all Col1a2 null groups at 8 weeks and n=5 for all Col1a2 null groups at 18. n=7 for all Col1a2 null groups at 52 weeks, except male +/- where n=5 and -/- where n=4.

Age-related deterioration of Col1a2 null male homozygotes

The tm1b line (Col1a2 null) was maintained on a mild protocol and mice exceeding the mild severity limited were legally required to be humanely killed. We noted an unexpectedly high loss of male Col1a2 null homozygotes due to a loss of condition, including weight loss and respiratory difficulties. A Kaplan-Meier 'survival' analysis was performed on the Col1a2 null mouse line (Fig. 6). All genotyped mice from this line were included in the analysis up to the age of 12 months, the end point for all experiments. The majority of genotypes had very few losses throughout the time course, with no animals lost for female wild-types and heterozygotes and only one animal lost for female homozygotes, male wild-types and heterozygotes out of a total of 19 mice. In contrast, almost 50% of male homozygotes were lost over the 12 month experimental period.

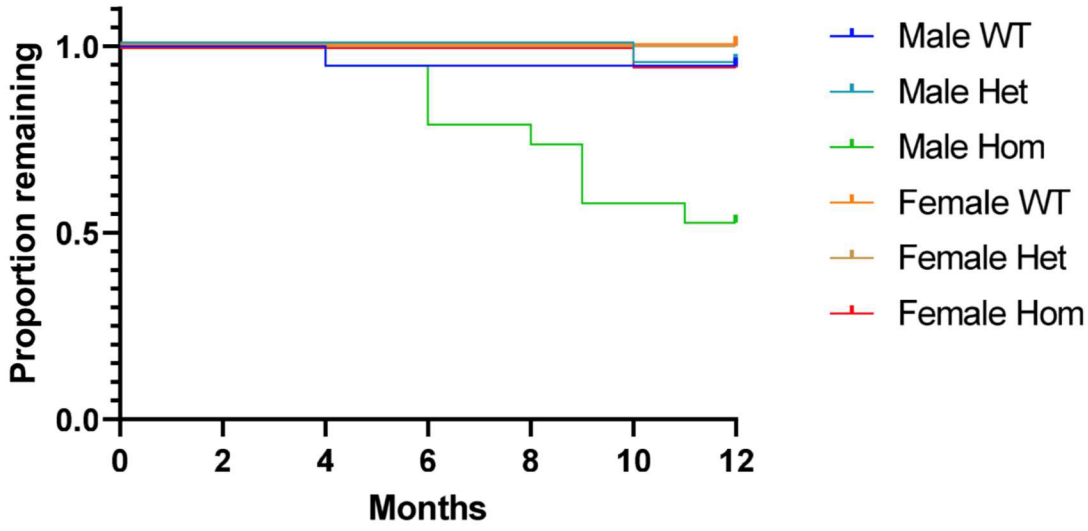

Figure 6. Survival analysis for the Col1a2KO mouse line. A Kaplan-Meier 'survival' analysis was performed on all genotyped mice from the Col1a2 null line up until 12 months (end of experiment). A log-rank (Mantel-Cox) test was performed which gave an overall p-value of <0.0001 indicating a significant difference between survival curves. n=19 for all groups.

Oim heterozygotes do not down-regulate the mutant allele

We considered that the less severe bone phenotype of oim heterozygotes could be related to a compensatory down-regulation of mRNA from the oim mutant allele. A custom allelic discrimination assay indicated that mRNA from both alleles was present in bone tissue from heterozygotes at both 8 (Fig. 7A) and 18 weeks of age (Fig. 7B). Whilst other tissues can be affected in the oim line the bone phenotype is particularly severe. We therefore determined whether there was compensatory downregulation of the mutant allele in tendon at 8 weeks (Fig. 7C) and 18 weeks (Fig. 7D), and in aorta (Fig. 7E), kidney (Fig. 7F), liver (Fig. 7G), or lung (Fig. 7H) at 18 weeks. For all tissues examined, mRNA from both alleles was present at a close to 50-50% ratio in heterozygotes.

Over page:

Figure 7. Allelic discrimination in the oim line. Allelic discrimination was carried out in bone (A-B) and tendon (C-D) at 8 (A, C) and 18 weeks (B, D) and in aorta (E), kidney (F), liver (G) and lung (H) at 18 weeks using ROX labelled primer/probes for the wild-type and VIC for the oim allele channels. For all tissues wild-types displayed little to no VIC signal, whilst homozygotes displayed no ROX signal. Heterozygotes had approximately intermediate signals in both channels with no systematic deviations between sexes or tissues. n=4 for all groups except 8 week bone and tendon samples from male and female oim/oim where n=2-3, 18 week bone and tendon samples from male +/+ where n=5 and female +/oim where n=1, kidney, aorta and lung samples for female +/+ and +/oim where n=3.

A

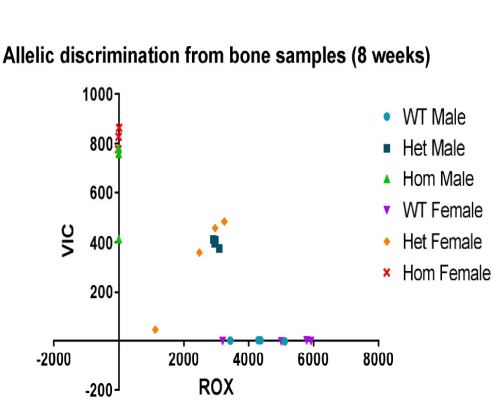

B

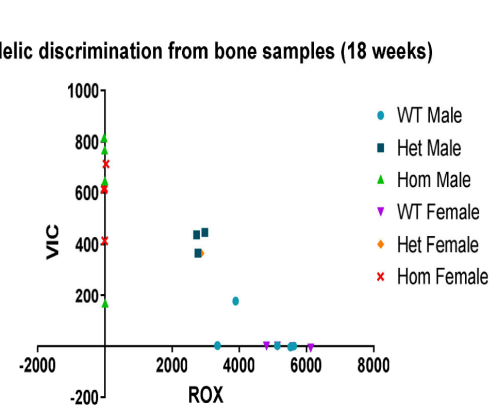

C

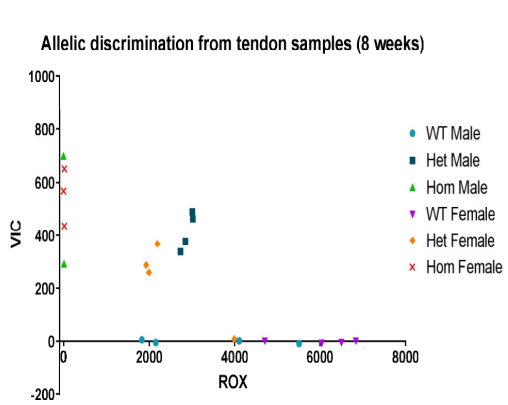

D

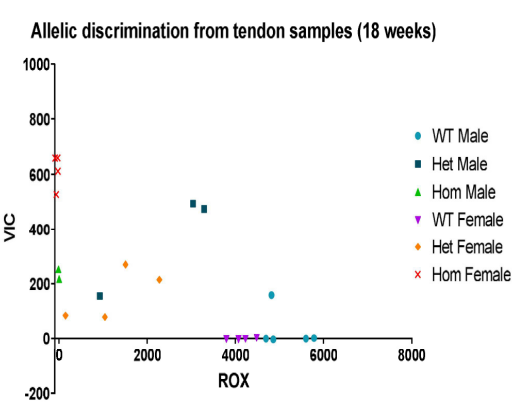

E

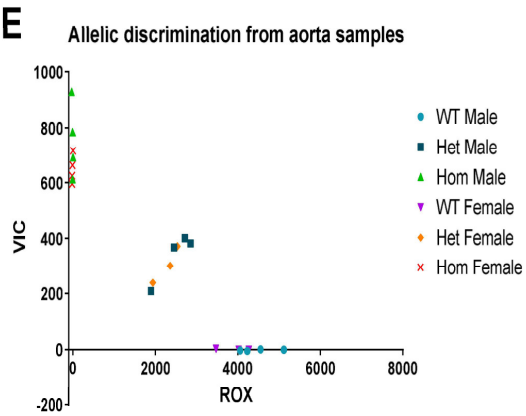

F

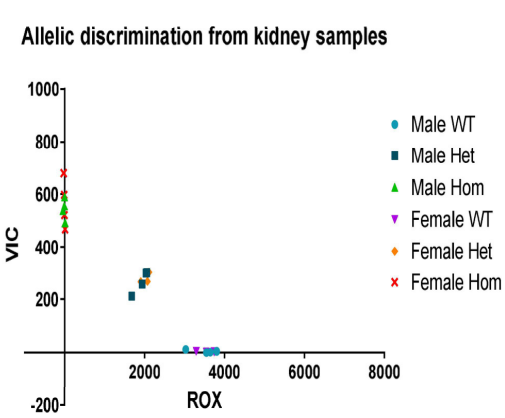

G

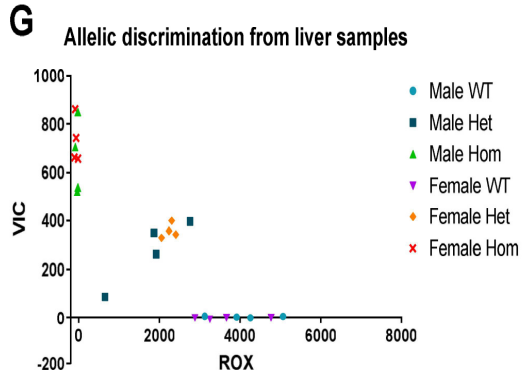

H

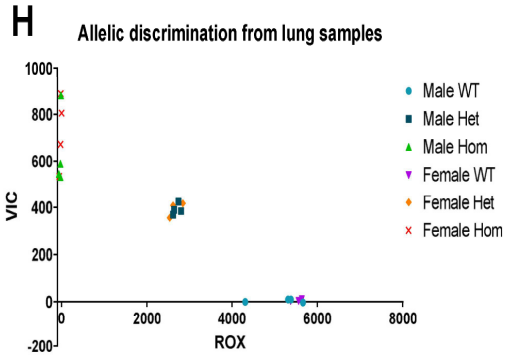

498

There is a genetic interaction between the oim mutant allele and collagen (I) homotrimer

As the mutant allele is not downregulated in oim heterozygotes, it is feasible that the less severe phenotype relates to gene dosage; given that heterozygotes have 1 rather than 2 copies of the mutant allele. To test this hypothesis we crossed the oim and tm1b lines to produce compound heterozygote offspring, along with heterozygotes of each genotype (Fig. 8A). Compound heterozygotes contain only one copy of the oim mutant allele but have no wild-type Col1a2 allele so produce solely homotrimeric α1 type I collagen.

The proximal tibias from 8-week-old oim and Col1a2 null (oim/Col1a2 null) cross line mice were analysed by µCT (Fig. 8 B-G). Oim/Col1a2 null compound heterozygotes demonstrated a significantly reduced bone volume (Fig. 8B), trabecular thickness (males only) (Fig. 8C), trabecular number (Fig. 8E) and an increased trabecular separation (Fig. 8D), compared with wild-types, Col1a2 null heterozygotes and oim heterozygotes. Connectivity was reduced in male compound heterozygotes compared to Col1a2 null heterozygotes (Fig. 8F). Therefore the phenotype of the compound heterozygote was more severe than that of the oim heterozygotes, indicating that gene dosage alone does not determine phenotypic severity.

The data for the compound heterozygotes was compared to that of the oim homozygotes and the Col1a2 null line, all of which produce no heterotrimeric type I collagen (Fig. S1). Oim homozygotes and compound heterozygotes demonstrated a reduced bone volume (Fig. S1A), trabecular thickness (males only) (Fig. S1B), trabecular separation (Fig. S1D) and connectivity (males only) (Fig. S1E), compared to Col1a2 null homozygotes. Trabecular separation was significantly increased in oim homozygotes compared to Col1a2 null homozygotes and compound heterozygotes (Fig. S1C). There was also a significant difference between female compound heterozygotes and Col1a2 null homozygotes. Male oim homozygotes demonstrated reduced BV/TV, trabecular thickness, trabecular number and connectivity and increased trabecular separation compared to compound heterozygotes. Fewer differences were seen for females with only an increased trabecular separation observed in oim homozygotes compared to compound heterozygotes. Therefore the bone phenotype of the compound heterozygotes was considerably more severe than the Col1a2 null lacking any mutant α2(I) chain, but less severe than the oim homozygotes with two mutant alleles.

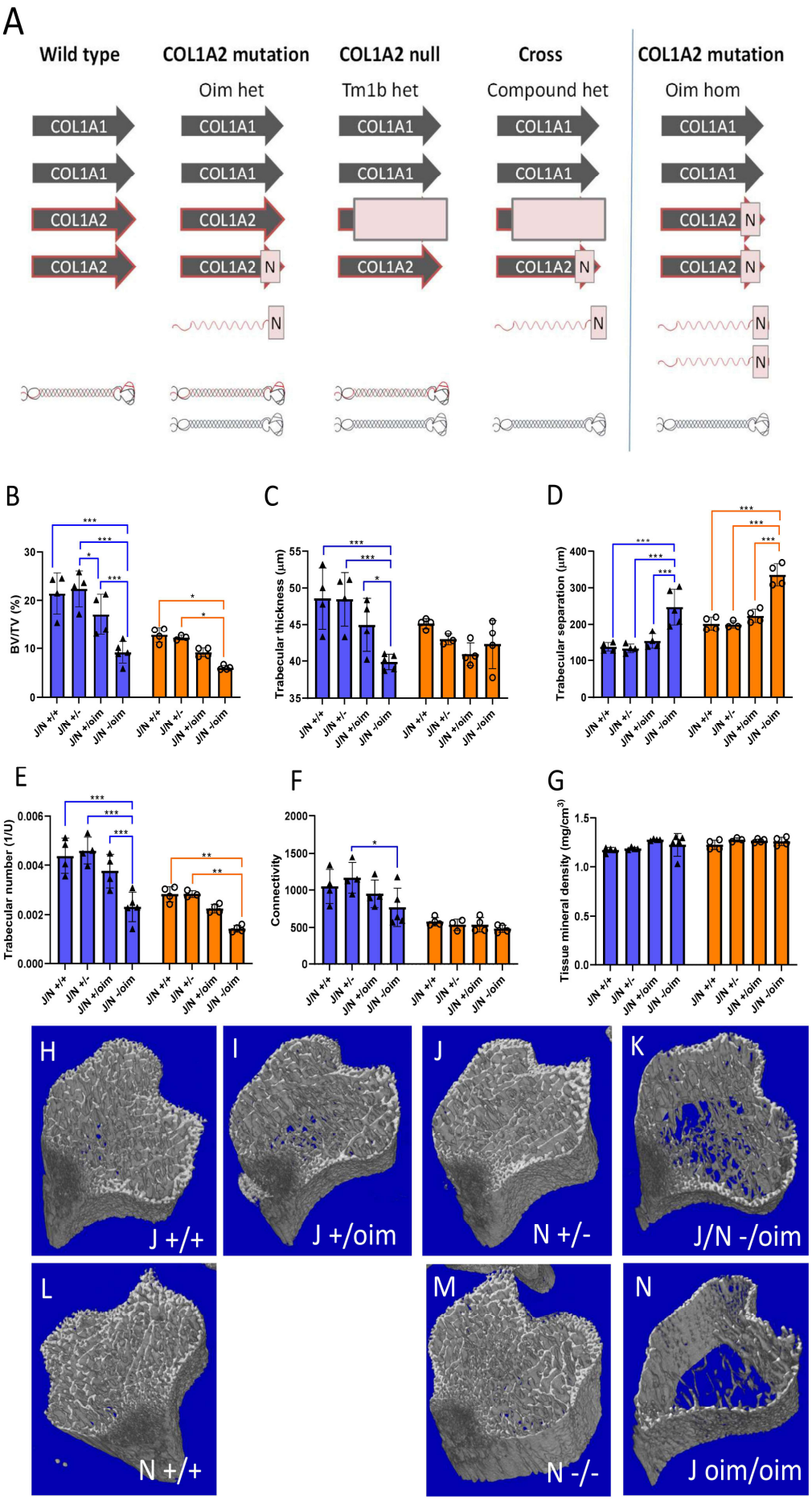

Figure 8. Bone structural properties are impaired in compound heterozygotes as compared to heterozygotes of the oim or Col1a2 null lines. A: Genetic differences between the heterozygous oim and Col1a2 null alleles and the compound heterozygous allele, with implications for collagen (I) protein synthesis. The homozygous oim allele is shown for comparison. Arrows indicate COL1 genes; N indicates mutation, light red box indicates null allele. Folded heterotrimeric proteins are indicated in black and red, whilst homotrimers are in black only. The presence of unincorporated mutant Col1a2 allele is indicated as a red waveform with a mutation (N). B-G: MicroCT scans were performed on the knee joints of offspring from heterozygous crosses of each line. Reconstruction and analysis of scan files enabled determination of bone volume (B), trabecular thickness (C), trabecular separation (D), trabecular number (E), connectivity (F) and bone density (G). H-N: Representative scan images from wild-types from the oim line (H), oim heterozygotes (I), Col1a2 null heterozygotes (J), compound heterozygotes (K), wild-types from the Col1a2 null line (L), Col1a2 null homozygotes (M) and oim homozygotes (N). Bone structural defects are more pronounced in compound than in oim heterozygotes. Blue bars/triangles = males, orange bars/circles = females. Blue and orange bars show differences between genotypes. * = p-value < 0.05 and *** = p-value <0.001. Overall p-values from two-way ANOVA tests were <0.001 (genotype) and <0.001 (sex) for B, <0.001 (genotype) and 0.012 (sex) for C, <0.001 (genotype) and <0.001 (sex) for D, <0.001 (genotype) and <0.001 (sex) for E, 0.069 (genotype) and <0.001 (sex) for F, and the overall p-value from a Kruskall Wallis H test was 0.03 for G. n=4 for all groups, except male oim/- where n=5 and female -/+ where n=3.

Discussion

To determine the contribution of collagen (I) homotrimer to bone fragility, we compared the bone phenotype of two mouse lines that lack the α2 chain of type I collagen: the oim mutant, a Col1a2 null and a combination of the lines. After propagating the lines, we measured a difference in Mendelian inheritance for males from both lines; interestingly this seemed to increase the proportion of wild-type males whilst decreasing the proportion of heterozygotes. To our knowledge pre-weaning loss of male heterozygotes has not been reported for either line. Enzymatic susceptibility assays and differential scanning calorimetry have previously indicated that tail tendon from heterozygous oim mice contains both heterotrimeric and homotrimeric type I collagen (Kuznetsova et al., 2003; McBride et al., 1997). Reconstituted fibrils comprising both heterotrimeric and homotrimeric collagen (I) molecules showed subfibrillar segregation of each trimeric form (Han et al., 2008). Hence, mixed fibrils in heterozygotes may affect tissue remodelling or mechanics during development resulting in decreased survival of heterozygotes.

Unlike oim homozygotes, we observed no fractures in Col1a2 null homozygotes. Bone structural parameters and material properties were largely similar between wild-type, heterozygote and Col1a2 null homozygotes. However, for males there was a decrease in bone volume and trabecular thickness at 8 weeks and a reduction in ultimate strength in tibia at 18 weeks in homozygotes as compared with wild-type, paralleling the trend but not the extent of the reduction observed in oim homozygotes. Our results for the oim line at 8 weeks are in agreement with previous studies showing a significant reduction in tibial bone volume and trabecular thickness in oim homozygotes (Ranzoni et al., 2016) and a significant reduction in ultimate strength and stiffness of the femur (Vanleene et al., 2011) .

By including sex as a factor in our analyses we noted the decrease in tibial trabecular thickness and femur stiffness was particular to male homozygotes. Our results for the oim line at 18 weeks were similar to those previously reported for 4 month old mice on the same background although with some differences relating to the significance or gender/sex dependence of the differences (Yao et al., 2013). In accordance with previous studies, we found no difference in intrinsic elastic modulus or ultimate stress in oim homozygotes (Vanleene et al., 2012; Vanleene et al., 2011; Yao et al., 2013) except for ultimate stress in male 18 week homozygotes. Decreased ultimate stress was previously reported for 12-14 week oim homozygotes (Bart et al., 2014; Miller et al., 2007), but not in all studies (Zimmerman et al., 2018). Oim homozygote mice were lighter and visually smaller than their wild-type and heterozygote littermates, therefore the differences seen in extrinsic but not intrinsic mechanical properties between oim homozygotes and wild-types could imply that the increased bone fragility of oim homozygotes is due to the reduced size of these mice. However, there were few significant differences in bone cross-sectional area between oim homozygotes and wild-types (only for tibias from 18 week old mice) and microCT analysis indicates the presence of intrinsic differences in bone structure with reduced cortical and trabecular bone.

Col1a2 null homozygotes did not display bone fragility but swollen joints were identified in males who also displayed age-related deterioration in condition. Human COL1A2 null homozygotes have cardiac valvular Ehlers-Danlos syndrome (cvEDS) (Guarnieri et al., 2019; Malfait et al., 2006) hence the age-related deterioration in mice may relate to cardiovascular abnormalities. Indeed the International Mouse Phenotyping Consortium reports dilated left heart ventricle measured at 12 weeks of age and increased heart weight at 16 weeks in Col1a2 null homozygotes (IMPC). Cardiovascular abnormalities were however observed in mice of both sexes and cvEDS patients are

not solely male. It may be that cardiovascular defects present earlier in male mice due to increased activity or remain subclinical in females. IMPC also reported a skeletal phenotype for Col1a2 null male mice with increased (notably not decreased) bone mineral content and density (DEXA, 14 weeks) and "abnormal" femur and tibia morphology (X-ray, 14 weeks). Reported phenotypes change over time due to continual addition of control samples ,but alterations to body fat in males and increased circulating alkaline phosphates in both sexes were also listed.

A key finding of this study was that the bone phenotype of a single copy of the oim allele was exacerbated by the absence of heterotrimeric type I collagen; i.e. that oim heterozygotes had a less severe phenotype than compound oim/null heterozygotes. Notably the phenotype of oim homozygotes still appeared more severe than that of compound heterozygotes, indicating some gene dosage effect for the mutant allele. Oim heterozygotes do not down-regulate the mutant allele (Fig. 7) hence presumably there is no mechanism to detect the oim mutation prior to translation or trimerization. We observed several significant differences between oim heterozygotes and wild-type controls, including reduced bone stiffness and increased trabecular separation in tibias from 18 week old female heterozygotes and reduced bone volume in 18 week old males. These results are contrary to a previous study which reported no significant differences for these parameters in a similar cohort of mice (Yao et al., 2013). Eight week old male heterozygotes also displayed reduced bone volume, trabecular thickness and connectivity compared to wild-type controls. In oim heterozygotes it is unclear if these observed differences in bone parameters as compared to wild-type controls relate solely to the interaction between the oim mutant allele and the proportion of homotrimeric collagen (I) that was present, or if the oim allele alone exerts an effect. The genetic interaction between the oim allele and homotrimeric collagen (I) could relate to the process of collagen folding and trimerization within the endoplasmic reticulum, or indeed the homotrimeric collagen (I) could alter cell-matrix interactions to modulate cellular stress responses. Procollagen N- and C-propeptides, derived from the proteolytic cleavage of procollagen, have been shown to have intracellular roles in modulating protein synthesis (Hayata et al., 2008; Marongiu et al., 2016; Oganesian et al., 2006) whilst homotrimeric triple helical regions increased proliferation and migration as compared to heterotrimeric pepsinised collagen (Makareeva et al., 2010). Hence homotrimeric forms of collagen fibrils or propeptides have the potential for altered signalling affecting cellular stress responses. The association of homotrimeric type I collagen with several common human age-related diseases, in which it is unlikely to predominate structurally, could therefore relate to altered cellular signalling or cell stress responses.

The experiments outlined above demonstrate a genetic interaction between homotrimeric collagen (I) and the oim mutant allele, suggesting that the presence of heterotrimeric collagen (I) in oim heterozygotes alleviates the effect of the oim mutant allele. The molecular basis of such interaction remains to be elucidated.

Author Contributions

KJL: Data curation, Formal Analysis, Investigation, Project administration, Supervision, Visualization, Writing – original draft, Writing – review & editing; LR: Data curation, Investigation, Visualization; GBG: Funding acquisition, Methodology, Writing – review & editing; PC: Conceptualization, Funding acquisition, Writing – review & editing; RA: Funding acquisition, Methodology, Writing – review & editing; GC: Formal Analysis, Funding acquisition, Writing – review & editing; RVH: Data curation,

Investigation, Funding acquisition, Investigation, Methodology, Software, Supervision, Visualization, Writing – review & editing; EGC-L: Conceptualization, Funding acquisition, Project administration, Supervision, Visualization, Writing – original draft, Writing – review & editing

Acknowledgements

The study was funded by the UK Medical Research Council (MR/R00319X/1). LR was supported by the Erasmus+ program.

References

Bailey, A.J., T.J. Sims, and L. Knott. 2002. Phenotypic expression of osteoblast collagen in osteoarthritic bone: production of type I homotrimer. *Int J Biochem Cell Biol*. 34:176-182.

Bart, Z.R., M.A. Hammond, and J.M. Wallace. 2014. Multi-scale analysis of bone chemistry, morphology and mechanics in the oim model of osteogenesis imperfecta. *Connect Tissue Res*. 55 Suppl 1:4-8.

Brull, D.J., L.J. Murray, C.A. Boreham, S.H. Ralston, H.E. Montgomery, A.M. Gallagher, F.E. McGuigan, G. Davey Smith, M. Savage, S.E. Humphries, and I.S. Young. 2001. Effect of a COL1A1 Sp1 binding site polymorphism on arterial pulse wave velocity: an index of compliance. *Hypertension*. 38:444-448.

Camacho, N.P., L. Hou, T.R. Toledano, W.A. Ilg, C.F. Brayton, C.L. Raggio, L. Root, and A.L. Boskey. 1999. The material basis for reduced mechanical properties in oim mice bones. *J Bone Miner Res*. 14:264-272.

Canty, E.G., and K.E. Kadler. 2005. Procollagen trafficking, processing and fibrillogenesis. *J Cell Sci*. 118:1341-1353.

Carleton, S.M., D.J. McBride, W.L. Carson, C.E. Huntington, K.L. Twenter, K.M. Rolwes, C.T. Winkelmann, J.S. Morris, J.F. Taylor, and C.L. Phillips. 2008. Role of genetic background in determining phenotypic severity throughout postnatal development and at peak bone mass in Col1a2 deficient mice (oim). *Bone*. 42:681-694.

Carriero, A., E.A. Zimmermann, A. Paluszny, S.Y. Tang, H. Bale, B. Busse, T. Alliston, G. Kazakia, R.O. Ritchie, and S.J. Shefelbine. 2014. How tough is brittle bone? Investigating osteogenesis imperfecta in mouse bone. *J Bone Miner Res*. 29:1392-1401.

Chessler, S.D., and P.H. Byers. 1993. BiP binds type I procollagen pro α chains with mutations in the carboxyl-terminal propeptide synthesized by cells from patients with osteogenesis imperfecta. *J Biol Chem*. 268:18226-18233.

Chipman, S.D., H.O. Sweet, D.J. McBride, Jr., M.T. Davisson, S.C. Marks, Jr., A.R. Shuldiner, R.J. Wenstrup, D.W. Rowe, and J.R. Shapiro. 1993. Defective pro α 2(I) collagen synthesis in a recessive mutation in mice: a model of human osteogenesis imperfecta. *PNAS*. 90:1701-1705.

DiChiara, A.S., R.C. Li, P.H. Suen, A.S. Hosseini, R.J. Taylor, A.F. Weickhardt, D. Malhotra, D.R. McCaslin, and M.D. Shoulders. 2018. A cysteine-based molecular code informs collagen C-propeptide assembly. *Nat Commun*. 9:4206.

Ehrlich, H.P., H. Brown, and B.S. White. 1982. Evidence for type V and I trimer collagens in Dupuytren's Contracture palmar fascia. *Biochem Med*. 28:273-284.

Forlino, A., W.A. Cabral, A.M. Barnes, and J.C. Marini. 2011. New perspectives on osteogenesis imperfecta. *Nat Rev Endocrinol*. 7:540-557.

709 Forlino, A., N.V. Kuznetsova, J.C. Marini, and S. Leikin. 2007. Selective retention and degradation of
710 molecules with a single mutant α1(I) chain in the Brtl IV mouse model of OI. *Matrix Biol*.
711 26:604-614.
712 Gioia, R., F. Tonelli, I. Ceppi, M. Biggiogera, S. Leikin, S. Fisher, E. Tenedini, T.A. Yorgan, T. Schinke, K.
713 Tian, J.M. Schwartz, F. Forte, R. Wagener, S. Villani, A. Rossi, and A. Forlino. 2017. The
714 chaperone activity of 4PBA ameliorates the skeletal phenotype of Chihuahua, a zebrafish
715 model for dominant osteogenesis imperfecta. *Hum Mol Genet*. 26:2897-2911.
716 Grabner, B., W.J. Landis, P. Roschger, S. Rinnerthaler, H. Peterlik, K. Klaushofer, and P. Fratzl. 2001.
717 Age- and genotype-dependence of bone material properties in the osteogenesis imperfecta
718 murine model (oim). *Bone*. 29:453-457.
719 Guarnieri, V., S. Morlino, G. Di Stolfo, S. Mastroianno, T. Mazza, and M. Castori. 2019. Cardiac
720 valvular Ehlers-Danlos syndrome is a well-defined condition due to recessive null variants in
721 COL1A2. *Am J Med Genet A*. 179:846-851.
722 Han, S., E. Makareeva, N.V. Kuznetsova, A.M. DeRidder, M.B. Sutter, W. Losert, C.L. Phillips, R. Visse,
723 H. Nagase, and S. Leikin. 2010. Molecular mechanism of type I collagen homotrimer
724 resistance to mammalian collagenases. *J Biol Chem*. 285:22276-22281.
725 Han, S., D.J. McBride, W. Losert, and S. Leikin. 2008. Segregation of type I collagen homo- and
726 heterotrimers in fibrils. *J Mol Biol*. 383:122-132.
727 Hayata, T., T. Nakamoto, Y. Ezura, and M. Noda. 2008. Ciz, a transcription factor with a
728 nucleocytoplasmic shuttling activity, interacts with C-propeptides of type I collagen. *Biochem*
729 *Biophys Res Commun*. 368:205-210.
730 IMPC. International Mouse Phenotyping Consortium: Col1a2.
731 https://www.mousephenotype.org/data/genes/MGI:88468. Date accessed: 8 June 2020.
732 Kerns, J.G., P.D. Gikas, K. Buckley, A. Shepperd, H.L. Birch, I. McCarthy, J. Miles, T.W.R. Briggs, R.
733 Keen, A.W. Parker, P. Matousek, and A.E. Goodship. 2014. Evidence from Raman
734 Spectroscopy of a Putative Link Between Inherent Bone Matrix Chemistry and Degenerative
735 Joint Disease. *Arthritis & Rheumatology*. 66:1237-1246.
736 Kuznetsova, N.V., D.J. McBride, and S. Leikin. 2003. Changes in thermal stability and microunfolding
737 pattern of collagen helix resulting from the loss of α2(I) chain in osteogenesis imperfecta
738 murine. *J Mol Biol*. 331:191-200.
739 Lees, J.F., M. Tasab, and N.J. Bulleid. 1997. Identification of the molecular recognition sequence
740 which determines the type-specific assembly of procollagen. *EMBO J*. 16:908-916.
741 Lisse, T.S., F. Thiele, H. Fuchs, W. Hans, G.K. Przemeck, K. Abe, B. Rathkolb, L. Quintanilla-Martinez,
742 G. Hoelzlwimmer, M. Helfrich, E. Wolf, S.H. Ralston, and M. Hrabe de Angelis. 2008. ER
743 stress-mediated apoptosis in a new mouse model of osteogenesis imperfecta. *PLoS Genet*.
744 4:e7.
745 Makareeva, E., N.A. Aviles, and S. Leikin. 2011. Chaperoning osteogenesis: new protein-folding
746 disease paradigms. *Trends Cell Biol*. 21:168-176.
747 Makareeva, E., S. Han, J.C. Vera, D.L. Sackett, K. Holmbeck, C.L. Phillips, R. Visse, H. Nagase, and S.
748 Leikin. 2010. Carcinomas Contain a Matrix Metalloproteinase–Resistant Isoform of Type I
749 Collagen Exerting Selective Support to Invasion. *Cancer Res*. 70:4366-4374.
750 Malfait, F., S. Symoens, P. Coucke, L. Nunes, S. De Almeida, and A. De Paepe. 2006. Total absence of
751 the α2(I) chain of collagen type I causes a rare form of Ehlers-Danlos syndrome with
752 hypermobility and propensity to cardiac valvular problems. *J Med Genet*. 43:e36.
753 Marongiu, M., M. Deiana, L. Marcia, A. Sbardellati, I. Asunis, A. Meloni, A. Angius, R. Cusano, A. Loi,
754 F. Crobu, G. Fotia, F. Cucca, D. Schlessinger, and L. Crisponi. 2016. Novel action of FOXL2 as
755 mediator of Col1a2 gene autoregulation. *Dev Biol*. 416:200-211.
756 McBride, D.J., Jr., V. Choe, J.R. Shapiro, and B. Brodsky. 1997. Altered collagen structure in mouse tail
757 tendon lacking the α 2(I) chain. *J Mol Biol*. 270:275-284.

758 Miller, E., D. Delos, T. Baldini, T.M. Wright, and N. Pleshko Camacho. 2007. Abnormal mineral-matrix
759 interactions are a significant contributor to fragility in oim/oim bone. *Calcif Tissue Int*.
760 81:206-214.
761 Mirigian, L.S., E. Makareeva, E.L. Mertz, S. Omari, A.M. Roberts-Pilgrim, A.K. Oestreich, C.L. Phillips,
762 and S. Leikin. 2016. Osteoblast Malfunction Caused by Cell Stress Response to Procollagen
763 Misfolding in α2(I)-G610C Mouse Model of Osteogenesis Imperfecta. *J Bone Miner Res*.
764 31:1608-1616.
765 Misof, K., W.J. Landis, K. Klaushofer, and P. Fratzl. 1997. Collagen from the osteogenesis imperfecta
766 mouse model (oim) shows reduced resistance against tensile stress. *J Clin Invest*. 100:40-45.
767 Nicholls, A.C., G. Osse, H.G. Schloon, H.G. Lenard, S. Deak, J.C. Myers, D.J. Prockop, W.R. Weigel, P.
768 Fryer, and F.M. Pope. 1984. The clinical features of homozygous α 2(I) collagen deficient
769 osteogenesis imperfecta. *J Med Genet*. 21:257-262.
770 Nicholls, A.C., F.M. Pope, and H. Schloon. 1979. Biochemical heterogeneity of osteogenesis
771 imperfecta: New variant. *Lancet*. 1:1193.
772 Oganesian, A., S. Au, J.A. Horst, L.C. Holzhausen, A.J. Macy, J.M. Pace, and P. Bornstein. 2006. The
773 NH2-terminal propeptide of type I procollagen acts intracellularly to modulate cell function.
774 *J Biol Chem*. 281:38507-38518.
775 Pace, J.M., M. Wiese, A.S. Drenguis, N. Kuznetsova, S. Leikin, U. Schwarze, D. Chen, S.H. Mooney, S.
776 Unger, and P.H. Byers. 2008. Defective C-propeptides of the proα2(I) chain of type I
777 procollagen impede molecular assembly and result in osteogenesis imperfecta. *J Biol Chem*.
778 283:16061-16067.
779 Pfeiffer, B.J., C.L. Franklin, F.H. Hsieh, R.A. Bank, and C.L. Phillips. 2005. A 2(I) collagen deficient oim
780 mice have altered biomechanical integrity, collagen content, and collagen crosslinking of
781 their thoracic aorta. *Matrix Biol*. 24:451-458.
782 Phillips, C.L., D.A. Bradley, C.L. Schlotzhauer, M. Bergfeld, C. Libreros-Minotta, L.R. Gawenis, J.S.
783 Morris, L.L. Clarke, and L.S. Hillman. 2000. Oim mice exhibit altered femur and incisor
784 mineral composition and decreased bone mineral density. *Bone*. 27:219-226.
785 Phillips, C.L., B.J. Pfeiffer, A.M. Luger, and C.L. Franklin. 2002. Novel collagen glomerulopathy in a
786 homotrimeric type I collagen mouse (oim). *Kidney Int*. 62:383-391.
787 Philp, A.M., R.L. Collier, L.M. Grover, E.T. Davis, and S.W. Jones. 2017. Resistin promotes the
788 abnormal Type I collagen phenotype of subchondral bone in obese patients with end stage
789 hip osteoarthritis. *Scientific reports*. 7:4042.
790 Prockop, D.J. 1988. Osteogenesis imperfecta. A model for genetic causes of osteoporosis and
791 perhaps several other common diseases of connective tissue. *Arthritis Rheum*. 31:1-8.
792 Ralston, S.H., A.G. Uitterlinden, M.L. Brandi, S. Balcells, B.L. Langdahl, P. Lips, R. Lorenc, B.
793 Obermayer-Pietsch, S. Scollen, M. Bustamante, L.B. Husted, A.H. Carey, A. Diez-Perez, A.M.
794 Dunning, A. Falchetti, E. Karczmarewicz, M. Kruk, J.P. van Leeuwen, J.B. van Meurs, J.
795 Mangion, F.E. McGuigan, L. Mellibovsky, F. del Monte, H.A. Pols, J. Reeve, D.M. Reid, W.
796 Renner, F. Rivadeneira, N.M. van Schoor, R.E. Sherlock, and J.P. Ioannidis. 2006. Large-scale
797 evidence for the effect of the COLIA1 Sp1 polymorphism on osteoporosis outcomes: the
798 GENOMOS study. *PLoS Med*. 3:e90.
799 Ranzoni, A.M., M. Corcelli, K.L. Hau, J.G. Kerns, M. Vanleene, S. Shefelbine, G.N. Jones, D.
800 Moschidou, B. Dala-Ali, A.E. Goodship, P. De Coppi, T.R. Arnett, and P.V. Guillot. 2016.
801 Counteracting bone fragility with human amniotic mesenchymal stem cells. *Scientific*
802 *reports*. 6:39656.
803 Rojkind, M., M.A. Giambrone, and L. Biempica. 1979. Collagen Types in Normal and Cirrhotic Liver.
804 *Gastroenterol*. 76:710-719.
805 Saban, J., M.A. Zussman, R. Havey, A.G. Patwardhan, G.B. Schneider, and D. King. 1996.
806 Heterozygous oim mice exhibit a mild form of osteogenesis imperfecta. *Bone*. 19:575-579.

Sharma, U., L. Carrique, S. Vadon-Le Goff, N. Mariano, R.N. Georges, F. Delolme, P. Koivunen, J. Myllyharju, C. Moali, N. Aghajari, and D.J. Hulmes. 2017. Structural basis of homo- and heterotrimerization of collagen I. *Nat Commun*. 8:14671.

Simon, M.M., S. Greenaway, J.K. White, H. Fuchs, V. Gailus-Durner, S. Wells, T. Sorg, K. Wong, E. Bedu, E.J. Cartwright, R. Dacquin, S. Djebali, J. Estabel, J. Graw, N.J. Ingham, I.J. Jackson, A. Lengeling, S. Mandillo, J. Marvel, H. Meziane, F. Preitner, O. Puk, M. Roux, D.J. Adams, S. Atkins, A. Ayadi, L. Becker, A. Blake, D. Brooker, H. Cater, M.F. Champy, R. Combe, P. Danecek, A. di Fenza, H. Gates, A.K. Gerdin, E. Golini, J.M. Hancock, W. Hans, S.M. Holter, T. Hough, P. Jurdic, T.M. Keane, H. Morgan, W. Muller, F. Neff, G. Nicholson, B. Pasche, L.A. Roberson, J. Rozman, M. Sanderson, L. Santos, M. Selloum, C. Shannon, A. Southwell, G.P. Tocchini-Valentini, V.E. Vancollie, H. Westerberg, W. Wurst, M. Zi, B. Yalcin, R. Ramirez-Solis, K.P. Steel, A.M. Mallon, M.H. de Angelis, Y. Herault, and S.D. Brown. 2013. A comparative phenotypic and genomic analysis of C57BL/6J and C57BL/6N mouse strains. *Genome Biol*. 14:R82.

Sims, T.J., C.A. Miles, A.J. Bailey, and N.P. Camacho. 2003. Properties of collagen in OIM mouse tissues. *Connect Tissue Res*. 44 Suppl 1:202-205.

Skarnes, W.C., B. Rosen, A.P. West, M. Koutsourakis, W. Bushell, V. Iyer, A.O. Mujica, M. Thomas, J. Harrow, T. Cox, D. Jackson, J. Severin, P. Biggs, J. Fu, M. Nefedov, P.J. de Jong, A.F. Stewart, and A. Bradley. 2011. A conditional knockout resource for the genome-wide study of mouse gene function. *Nature*. 474:337-342.

Sykes, B., B. Puddle, M. Francis, and R. Smith. 1976. The estimation of two collagens from human dermis by interrupted gel electrophoresis. *Biochem Biophys Res Commun*. 72:1472-1480.

Vanleene, M., A. Porter, P.-V. Guillot, A. Boyde, M. Oyen, and S. Shefelbine. 2012. Ultra-structural defects cause low bone matrix stiffness despite high mineralization in osteogenesis imperfecta mice. *Bone*. 50:1317-1323.

Vanleene, M., Z. Saldanha, K.L. Cloyd, G. Jell, G. Bou-Gharios, J.H. Bassett, G.R. Williams, N.M. Fisk, M.L. Oyen, M.M. Stevens, P.V. Guillot, and S.J. Shefelbine. 2011. Transplantation of human fetal blood stem cells in the osteogenesis imperfecta mouse leads to improvement in multiscale tissue properties. *Blood*. 117:1053-1060.

Vouyouka, A.G., B.J. Pfeiffer, T.K. Liem, T.A. Taylor, J. Mudaliar, and C.L. Phillips. 2001. The role of type I collagen in aortic wall strength with a homotrimeric. *J Vasc Surg*. 33:1263-1270.

Yao, X., S.M. Carleton, A.D. Kettle, J. Melander, C.L. Phillips, and Y. Wang. 2013. Gender-dependence of bone structure and properties in adult osteogenesis imperfecta murine model. *Ann Biomed Eng*. 41:1139-1149.

Zhong, B., D. Huang, K. Ma, X. Deng, D. Shi, F. Wu, and Z. Shao. 2017. Association of COL1A1 rs1800012 polymorphism with musculoskeletal degenerative diseases: a meta-analysis. *Oncotarget*. 8:75488-75499.

Zimmerman, S.M., M.E. Heard-Lipsmeyer, M. Dimori, J.D. Thostenson, E.M. Mannen, C.A. O'Brien, and R. Morello. 2018. Loss of RANKL in osteocytes dramatically increases cancellous bone mass in the osteogenesis imperfecta mouse (oim). *Bone Rep*. 9:61-73.

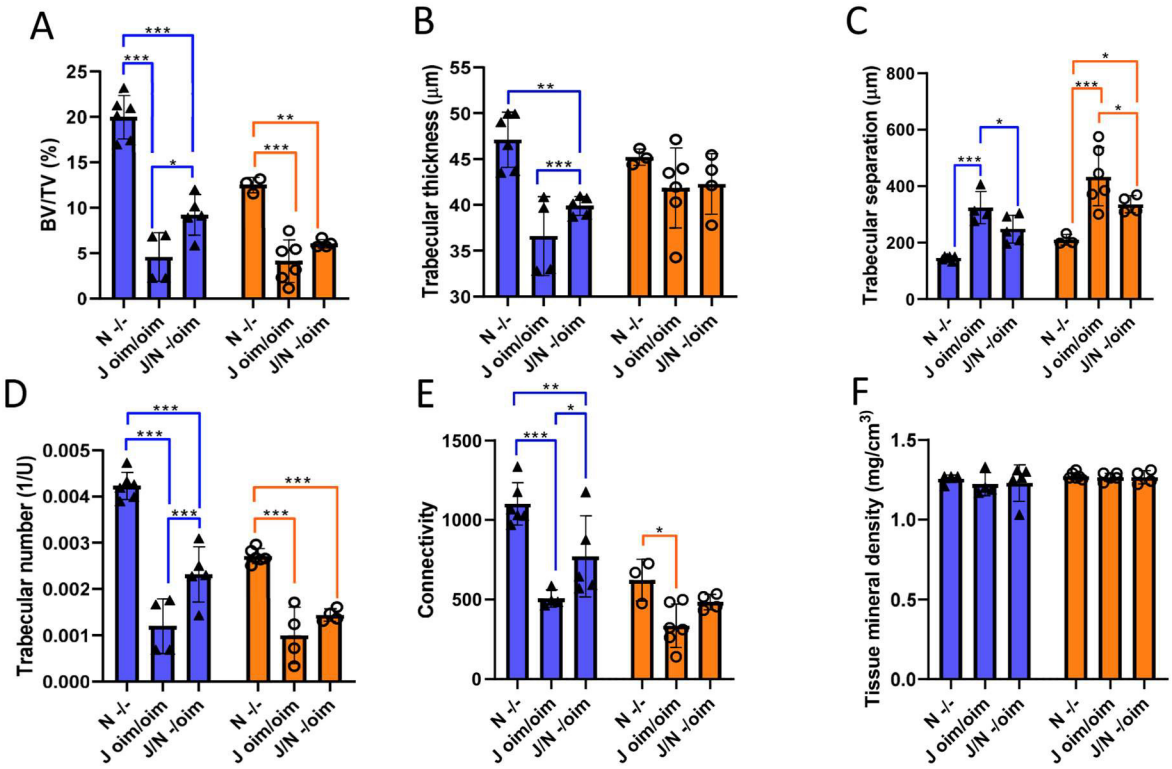

Figure S1. Bone structural properties in compound heterozygotes are less severe than Col1a2 null homozygotes. Bone volume (A), trabecular thickness (B), trabecular separation (C), trabecular number (D), connectivity (E) and bone density (F) data were compared for Col1a2 null homozygotes (-/-), oim homozygotes (oim/oim) and compound heterozygotes (-/oim). Blue bars/triangles = males, orange bars/circles = females. Blue and orange bars show differences between genotypes. * = p-value < 0.05, ** = p-value <0.01 and *** = p-value <0.001. The overall p-values from two-way ANOVA tests were <0.001 (genotype) and <0.001 (sex) for A, <0.001 (genotype) for B, <0.001 (genotype) and <0.001 (sex) for C, <0.001 (genotype) and <0.001 (sex) for D, <0.001 (genotype) and <0.001 (sex) for E. n=4 for all groups, except male oim/- where n=5 and female oim/oim and -/- and male -/- where n=6.